2010 IEEE International Conference on Robotics and Automation
Anchorage Convention District
May 3-8, 2010, Anchorage, Alaska, USA

A New Theory and Methods for Creating Peristaltic Motion in a Robotic Platform

Alexander S. Boxerbaum, Hillel J. Chiel, and Roger D. Quinn

Abstract — **We have developed several innovative designs for a new kind of robot that uses peristalsis for locomotion, the same method that earthworms use, and report on the first completed prototype (Fig. 1). This form of locomotion is particularly effective in constrained spaces, and although the motion has been understood for some time, it has rarely been effectively or accurately implemented in a robotic platform. We address some reasons for this, including some common misconceptions within the field. We present a technique using a braided mesh exterior to produce fluid waves of motion along the body of a worm-like robot. We also present a new analytical model of this motion and compare predicted robot velocity to a 2-D simulation. Unlike previous mathematical models of peristaltic motion, our model suggests that friction is not a limiting factor in robot speed, but only in acceleration. The concept is highly scalable, and we present methods of construction at two different scales.**

I. Introduction

Soft-bodied invertebrates, such as leeches, worms, and slugs, have successfully colonized marine, terrestrial, and fossorial (underground) environments. They do so with complex structures that can rapidly change shape on command. Some of these animals contain a central fluid-filled cavity. Contraction of a muscle component of the cavity induces an expansion of other parts of the cavity and of its surrounding muscle. Animals with these body architectures have a *hydrostatic skeleton* [1]. However, other soft structures, such as tongues, trunks, or tentacles, have higher power-to-mass ratios. These consist solely of muscle fibers with no central fluid-filled cavity and have been termed *muscular hydrostats* [2]. By deploying muscle groups arranged in ordered configurations—longitudinally, circumferentially, or helically—these structures are capable of both rapid and dexterous movements. The skins of soft-bodied animals have many sensors embedded within them. Their nervous systems coordinate their many degrees of freedom in order to locomote in a variety of ways, including peristaltic crawling, anchor-and-extend, and swimming [3]. Robots with similar capabilities would be able to complete many useful tasks, including reconnaissance through small crevices, exploring complex terrain for search and rescue missions, actively pushing an endoscope throughout the entire gastro-intestinal (GI) tract, or minimally invasive surgery. Serpentine robots have had the most success in some of these areas [4],[5], but rely on a motion that does not work as well in the most confined spaces where burrowing is required.

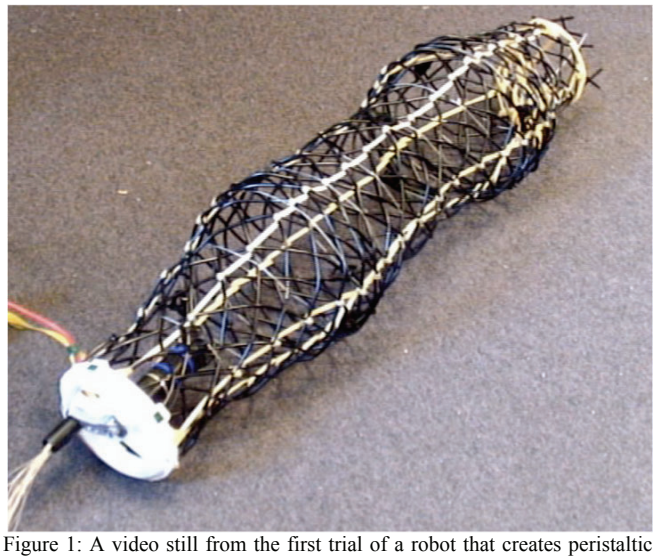

Figure 1: A video still from the first trial of a robot that creates peristaltic motion with a continuously deformable exterior surface.

Our group at Case Western Reserve University previously developed a worm robot using long braided pneumatic actuators (artificial muscles) in series (Fig. 2) [6]. A braided mesh was used to create a material with anisotropic strain properties. Compression along one axis caused expansion in another. In this case, the material was woven into a cylindrical shape and a bladder inflated the cylinder, pushing outward radially, which caused axial contraction. Despite the novel use of these air muscles, this robot had much in common with most robots attempting peristaltic motion: a minimal number of identical segments attached in series that each can alternately contract axially and expand radially [7]–[10]. In these robots, the area in between each segment is without actuation. This approach would be more suited to modeling animals that do have large segments, such as caterpillars [11]. A notable exception is an amoeba inspired robot by Hong and Ingram that doesn't use peristaltic motion, but has a novel whole-body method of locomotion [12].

Our previous robot moved much slower than expected, even for a worm-like robot. It would often appear to slip backwards, or have difficulty progressing when an obstacle landed between actuators. The slipping, which may be common among all robots attempting peristaltic motion, led

Manuscript received September 15, 2009. This work was supported in part by Roger D. Quinn, Hillel J. Chiel, and Kenneth Loparo.

Alexander S. Boxerbaum is with the Department of Mechanical and Aerospace Engineering, Case Western Reserve University, Cleveland, OH 44106-7222 USA (Phone: 216-952-2641, email: asb22@cwru.edu).

Hillel J. Chiel is with the Departments of Biology, Neurosciences, and Biomedical Engineering, Case Western Reserve University, Cleveland, OH 44106-7080 USA (email: hjc@case.edu).

Roger D. Quinn is with the Department of Mechanical and Aerospace Engineering, Case Western Reserve University, Cleveland, OH 44106-7222, USA (email: rdq@case.edu).

Figure 2: (Left) A previously built worm-like robot with discrete actuators surrounded by a braided mesh. (Right) The inner actuator core that inflates the mesh [6].

us and many others to conclude that friction was important for this mode of locomotion [8],[9]. Also, the robot's power requirements were substantial: it required an off-board pressurized air supply. These issues were the impetus for re-evaluating our understanding of peristaltic motion and its implementation in a robotic platform.

Earthworms have continuous sheets of both axial and circumferential muscle fibers that work together to create waves of peristaltic motion. During forward locomotion, these two muscle groups are coupled by segments of hydrostatic fluid and typically alternate activation at a given location along the body. In our new concept, we use a braided mesh similar to that used in pneumatically-powered artificial muscles [13] to create this coupling between axial and radial motion with a single hoop actuator. The robot is still cylindrical in shape, but the outer wall consists of a single continuous braided mesh (Fig. 1). Any location along the braided mesh can be fully expanded or contracted. Hoop actuators are located at intervals along the long axis, close enough together that smooth, continuous waves can be formed. When these hoop actuators are activated in series, a waveform travels down the length of the body. The result is a fluid motion more akin to peristaltic motion than that generated by previous robots.

II. Theory of Peristaltic Locomotion

Peristaltic locomotion has several interesting, counter-intuitive properties. The waves of expansion and contraction flow in the opposite direction of the robot motion. This is a direct result of the anisotropic strain properties of the body. When a section leaves the ground, a new ground contact point forms directly behind it. The contracting section will accelerate outward axially, but that motion is constrained on the rear side by the new ground contact point, so the segment must move forward (see the attached video for examples of this motion). Nonetheless, while the sections leaving ground contact are expanding axially, and accelerating forward, the sections making ground contact are decelerating at the same rate (even if the wave is asymmetric, the net accelerations and decelerations over the wave must cancel). Therefore, on flat ground, a robot with a whole number of waves traveling at a constant speed will have no need for friction forces in order to maintain a constant velocity. In this way, the motion is analogous to a wheel rolling on flat ground: points along the circumference are accelerating, but the wheel rolls at a constant velocity and requires no external forces. This means that peristaltic motion has the possibility of being very efficient, and may not be as constrained by the need for good ground friction as previously thought. This also suggests that another explanation is needed as to why robots attempting this motion frequently slip backwards.

A. Analytical Models:

An analytical model of peristaltic motion would be useful in many ways. It could provide insights for producing faster robots, and may eventually play a key part in a high level control strategy. A model was developed by Quillin to examine the kinematic scaling of earthworm locomotion [14] that has been used to predict robot speed by other groups. This model describes the speed of the worm or robot as:

$$\text{Speed} = \frac{\text{Stride Length}}{\text{Cycle Time}} \qquad (1)$$

While this observational model accurately characterizes earthworm locomotion on flat ground, it does not capture or explain the causes of slippage, and therefore tends to overestimate the speed of worm-like robots. To address this problem, we have developed a new analytical model of peristaltic motion that can deal with continuously deformable structures. We begin by finding the kinematics of an ideal continuous anisotropic material, and then derive equations for the robot position as a function of the waveform that travels along it. If the speed of the waveform is known, we can find the position and velocity of the robot as a function of time. Later, a specific waveform generator will be added to the model that approximates a cam mechanism that has been built.

B. Basic Four-bar Mechanism Derivation of Strain:

The mechanical strain that occurs with the simple braided mesh described above can be directly calculated from the geometry of four crossing strands (Fig. 3). We will assume the strands are rigid in order to treat them as a four-bar

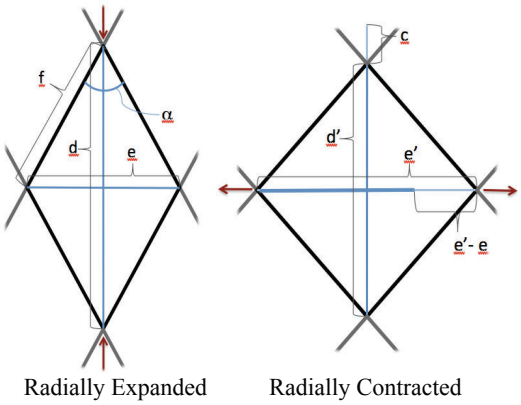

Figure 3: A single element of the braided mesh can be used to derive the anisotropic strain properties of the material. The dimension c' is the input, the change in length due to the hoop actuator.

mechanism. However, there must be bending in these fibers in order for distinct waves to form. The scale of the weave is not important for this derivation, as it only describes the anisotropic properties of a continuous ideal material. The hoop actuator contracts along *d,* changing its length to *d′*. The dimension along *e* will expand by an amount that is a function of the initial shape of the diagonal element, defined here by the angle α. From the Pythagorean theorem and the law of sines, we have:

$$d'^2 + e'^2 = (2 * f)^2 \rightarrow e' = \sqrt{(2 * f)^2 - d'^2} \quad (2)$$

$$\frac{f}{\sin(\pi/2)} = \frac{\frac{d}{2}}{\sin(\pi/2 - \alpha/2)} \rightarrow f = \frac{d}{2 * \cos(\alpha/2)} \quad (3)$$

The change in length along *d* is due to the hoop actuator displacement, *c*:

$$d' = (d - c) \quad (4)$$

The input *c* is often a periodic function that describes the contractions as a function of time or position. The two values *d′* and *c* must be scaled appropriately. For instance, if *c* is the total displacement of the hoop actuator over the circumference, then *d′* is the maximum circumference of the entire braided mesh.

The above equations can be combined to find the new axial length *e′*:

$$e' = \sqrt{\left(\frac{d}{\cos(\alpha/2)}\right)^2 - (d - c)^2} \quad (5)$$

Lastly, for the purposes of this analysis we will define the strain of the material as:

$$\varepsilon = \frac{e' - e}{e}, \quad (6)$$

where

$$e = d * \tan(\alpha/2) \quad (7)$$

Combining (5), (6), and (7) we now have an equation for the axial strain of the braided mesh as a function of the hoop actuator activation *c* and the geometry of the mesh defined by *d* and α:

$$\varepsilon = \frac{\sqrt{\left(\frac{d}{\cos(\alpha/2)}\right)^2 - (d - c)^2} - d * \tan(\alpha/2)}{d * \tan(\alpha/2)} \quad (8)$$

We will see that a strain function of this kind plays a critical role in determining the motion of the robot or animal.

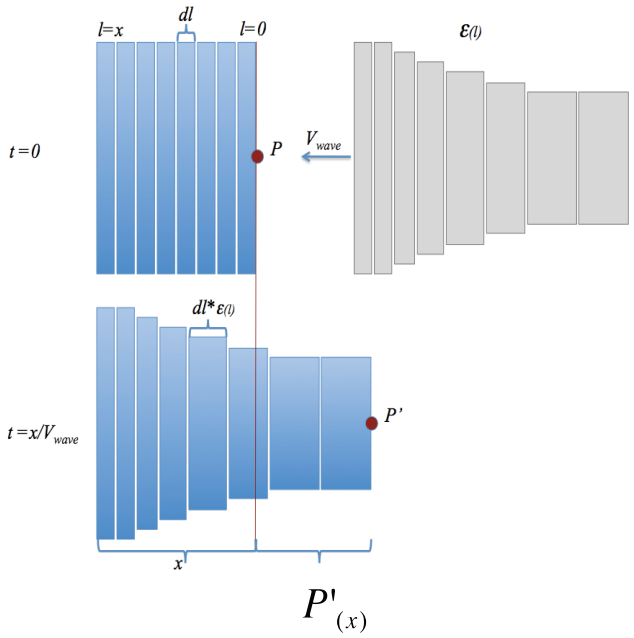

Figure 4: Illustration showing the new position of a point as the waveform travels through the body. The displacement can be found by integrating the strain function.

C. Derivation of Position as a Function of Time:

Let us consider a differential axial element on the front of the robot (Fig. 4). The element's initial displacement from its original position is first just the axial strain of that element caused by the wave. However, in the next moment, its displacement will also include the axial strain of the next differential element entering the wave. Therefore, the total displacement of the first element can be described as the integral of the strain as a function of length, *l*:

$$P'_{(x)} = \int_{l=0}^{l=x} \varepsilon(l)\,dl \quad (9)$$

If the deformation wave as a whole has a constant velocity, the position of a point *P* in global coordinates can be found as a function of time by replacing *x* with $t*V_{wave}$ and *dl* with $dt*V_{wave}$. Now,

$$P_{(t)} = \int_{0}^{T} \varepsilon(t * V_{wave})\,dt * V_{wave} \quad (10)$$

Also, since the velocity of the point *P* is the time derivative of (10),

$$V_{(t)} = \varepsilon(t * V_{wave}) * V_{wave} \quad (11)$$

These units are consistent because the output of the strain function is dimensionless. Equation 11 tells us that the speed of a point on the robot, and, by extension, the robot's speed, is a function of the shape of the deformation wave ε and the speed of this wave. Increasing the local deformation

(anisotropic strain) or increasing the wave speed will make the robot go faster.

Since both position and velocity of a point on the robot are functions of the strain wave deformation defined in Equation 9, once a hoop actuator path is prescribed, we can calculate position and velocity as a function of time.

III. 2-D Dynamic Simulation

A simple 2-D dynamic simulation was created to evaluate this method of locomotion, and to capture the discrete nature of individual segments that are not represented in the analytical model (Fig. 5). Each body segment consists of a modified four-bar mechanism, where each bar is split into two pieces joined by a torsional spring. This approximates the ability of the braided mesh to bend, an essential capability for wave formation. There are ten actuators, each driven by an identical periodic function derived from a cam mechanism discussed later. One of the advantages of this simulation is easy access to a large amount of data, including the positions, velocities, and accelerations of points on the robot, including its center of mass.

Because this simulation does not have a continuous exterior wall like our current prototype, the ground contact transitions are typically not smooth. Therefore, even with ten actuators, this simulation is similar to robots with defined segments. Some of the problems with this are discussed later when comparing this model to the analytical approach.

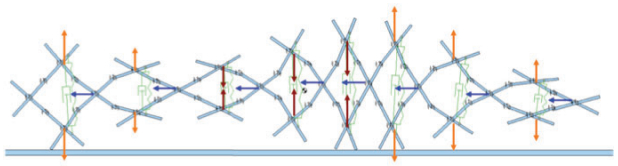

Figure 5: A simple 2-D simulation of the robotic concept. Orange arrows indicate hoop actuators that are expanding. Dark red arrows indicate hoop actuators that are contracting. Blue arrows indicate the resultant motion of the robot.

IV. Robotic Concepts at a Small Scale

The kinematics of peristaltic motion are entirely scale invariant. At any given scale, a cross-hatched mesh needs to be constructed with the correct stiffness, and a suitable actuation method found. Here, we briefly propose two methods of construction at a very small scale.

A. Shape Memory Alloys:

A robot with a diameter on the order of one centimeter would have applications in medicine, including examination of the entire GI tract, as well as applications in search and rescue environments and military reconnaissance. Shape Memory Alloys (SMAs) are a good candidate for actuation at this scale. Micro helix SMAs have strain ratios of up to 200% and can be actuated in under a second. The SMA could be wrapped around the robot and actuated by wiring that also constitutes the braided mesh (Fig. 6).

At this small scale, it may be advantageous to use a

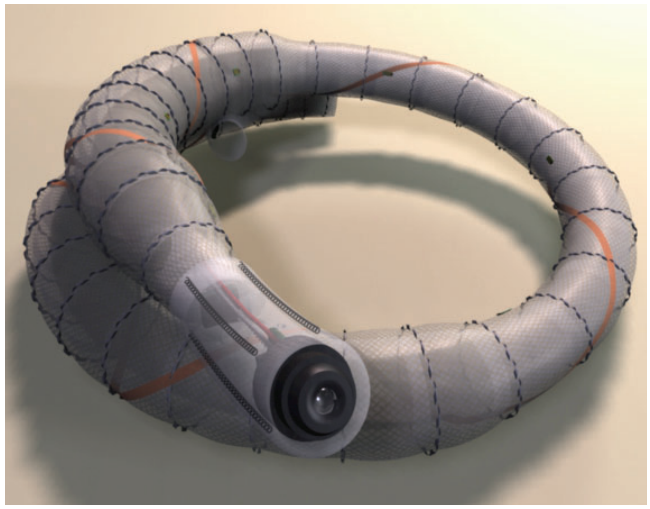

Figure 6: SoftWorm robotic concept using shape memory alloys and a hydrostatic fluid as a return spring.

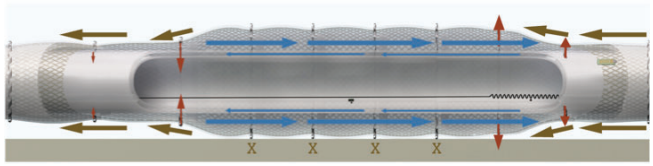

Figure 7: A cross sectional view of the SMA concept. The brown arrows indicate the flow of the exterior braided mesh. The blue arrows indicate the flow of the bolus of fluid that expands the contracted sections. The red arrows indicate expanding and contracting hoop actuators.

hydrostatic fluid to expand already contracted actuators. In this implementation, shown in Figure 7, a bolus of fluid (large blue arrows) moves between the outer skin and the inner payload of the robot by the sequential constriction of hoop SMA actuators (red inward-pointing arrows). As the fluid is squeezed at the trailing edge of the wave, it causes radial expansion at the leading edge of the wave (red outward-pointing arrows). The result is the generation of continuous peristaltic waves along the robot, causing it to move in the opposite direction of the wave (brown arrows).

B. Hydrostatic Fluid Actuators:

An alternative method of actuation at this small scale is being explored as well. The braided mesh of the robot could be made of hollow tubing and serve as hydraulic lines for micro-hydraulic actuators at each hoop (Fig. 8). Hydraulic actuators are generally only effective as pushing actuators, requiring the natural state of the robot to be elongated and narrow. Expansion at one of the hoop actuators would be achieved by applying pressure at the end of the hydraulic

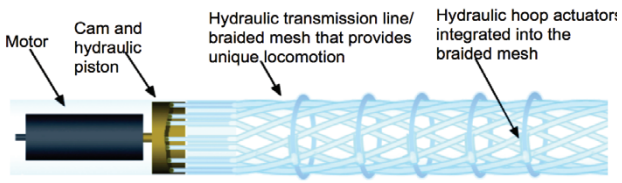

Figure 8: Micro-hydraulic actuator concept. Here, the hoop actuators expand against a contractile force to create the wave motion.

line. This would also allow for mechanical coupling of the hoop actuators, and allow them to be driven by a single end-mounted motor. This setup could achieve faster waves, and therefore faster robot speeds than the SMA implementation, but requires an effective micro-hydraulic piston to be developed.

V. Robotic Concepts at a Large Scale

Current Prototype:

A large scale prototype has recently been completed and tested. With a maximum diameter of 25 cm, it is scaled to function in water mains (Fig. 1). With its hollow core, it would be possible to service them without shutting off flow. Instead of relying on a hydrostatic fluid as a return spring, it is easier to use a series of mechanical springs (latex rubber tubing) at this scale.

The braided mesh that provides the unique anisotropic strain properties has an elegant dual function. It is made of brake cable sheathing and steel cables run through the sheathing out to individual hoop actuators. At these locations, there is a mechanism that interrupts the brake cable sheathing and routes the cable around the circumference (Fig. 9). This mechanism also holds the strand of sheathing that continues as the braided mesh for the rest of the length of the robot. Two cables run through a single sheathing and split in opposite directions to meet on the far side. This doubles the stroke length of the actuator compared to a single cable wrapped around the whole circumference. Small wire guides are attached along the hoop actuator path to keep it in place when it is not being contracted.

At the end of the robot, the steel actuator cables are pulled in sequence by a cam driven by a single drive motor (Fig. 10). While future versions may have individually controlled actuators in order to study sensorimotor wave propagation and adaptive behavior, this mechanism creates peristaltic motion with no computational overhead and with a waveform that provides good speed. In this way, forward and backward motion is controlled as a single degree of freedom using a single motor.

The cam mechanism is designed to pull on the cables with a waveform that is roughly sinusoidal in both time and space. The exact waveform is a combination of both sine and cosine waves that has a near singularity due to the geometry (Fig. 11). The shape of the waveform can be changed easily by changing the cam arm length (Fig. 10, line *b*). In the current setup two waves are present at all times. Closely paired cables visible in Figure 10 are routed to two hoop actuators spaced apart by half the length of the robot. Their proximity to each other on the perimeter of the cam indicates that these two actuators will have nearly identical states at any given point in time. Ten actuators are distributed along the length of the robot. However, ten additional actuators could be easily added by utilizing the remaining empty brake cable sheathings to either smooth out the wave, or to make the robot longer.

At first, we attempted to use polyester string as an actuator cable, because of its very small minimum bending

Figure 9: A hoop actuator created by a steel cable that runs through the brake cable sheathing.

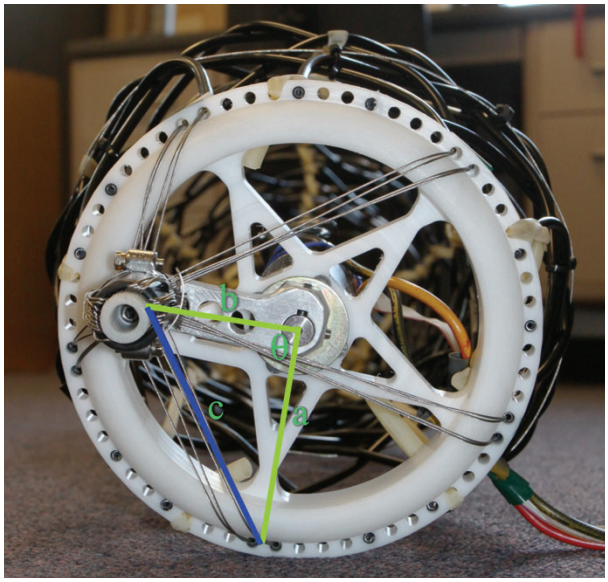

Figure 10: The cam mechanism that drives all actuators and creates two traveling waves along the length of the robot. The origin of the cables indicates their phase shift relative to the other actuators. The actuation length of this mechanism can be described with the law of cosines.

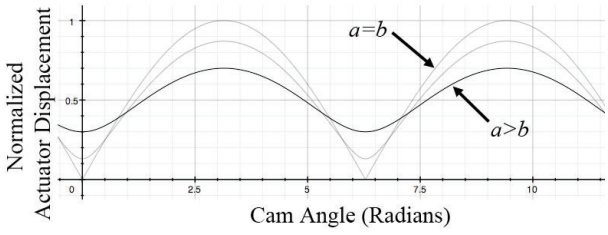

Figure 11: Three waveforms created by the cam mechanism. The greater the distance between the cam head and the axis of rotation, the sharper the lower transition.

radius. These strings repeatedly broke under loading. While Kevlar or Spectra string may still be good alternatives, we decided to use steel cable, specifically for its strength and its natural pairing with the brake cable sheathing, which was designed to interface with such a cable. The larger minimum bending radius of steel cable meant that special care had to be given to how the cables were routed. The final mechanism routes the cables such that the minimum bending radius is never less than 12 mm, sufficient to accommodate any steel cable small enough to fit in the brake cable sheathing.

Currently, the woven mesh maintains its shape due to the actual braiding of the strands of sheathing. The latex tubes that act as return springs also anchor the mesh together at points where they wrap around it. This is adequate for testing purposes, but deformations of the mesh have been regularly observed and need to be manually fixed. Future versions will have small joints at each strand juncture to align the sheathing and the hoop actuator cables. Alternatively, encasing the braided mesh in a soft polymer skin would also preserve the alignment of the strands and act as a return spring.

VI. Results and Discussion

A. Current Prototype:

The current prototype generates the desired waveforms successfully for short periods of time (see video). The robot has moved 120 cm forward in a single trial during initial testing. The speed was intentionally slow in order to help diagnose problems. Nonetheless, a speed of 0.97 m/min was achieved over a distance of 0.9 meters. The resolution of several minor mechanical problems will allow for longer testing, much higher speeds, and validation of our simulation and analytical models.

The primary mechanical problem is the securing of the actuator cables. The two most distant actuators require the most force to actuate because of their long runs through the brake cable sheathing. The cable clamping mechanism built into the cam head (Fig. 10) is often not strong enough to resist these high forces. So, typically after a few waveforms have passed through, the cables slip out, causing the most distant actuators to fail. Even with several failed actuators, the robot still moves forward at a slower speed. The cause of the variations in force between the actuator cables is the distance traveled in the sheathing. Therefore, the cable sections that actually contract the hoop actuator experience the same low forces regardless of the distance from the cam head. In the next version of the robot, the cable will be secured at the hoop actuator, rather than at the cam head. This should entirely eliminate the cable slipping problem. Also, the friction that is generated in the brake cable sheathing increases faster than linearly with length. Therefore, at smaller scales, the friction may be less significant relative to the otherwise required motor torque.

B. Analytical Model and Simulation:

An interesting effect was observed during the swing-stance transitions in the simulation of a segmented robot that might account for some of the challenges of building a segmented worm-like robot. When the ground contact point switches from one segment to the next, the second segment will contact the ground before it has fully expanded. Therefore, after ground contact, it will continue to contract axially, instead of expanding. This means that the wave gets unnaturally stretched due to too many constraints, and at least one of the ground contact points must slip.

Furthermore, because the new ground contact point is not formed soon enough, the segment that is leaving the ground loses the forward progress it would have made at the beginning of the swing phase. The analytical model shows that the acceleration of the segment would be greatest during this lost swing time, so the loss of speed is significant. Figure 12 is derived from Equation 9 and shows that given a set displacement, c, the initial angle α is a critical factor in the amount of axial strain that is achieved. While the most strain is achieved with small start angles, the forces required to move are high, due to the low mechanical advantage. Because the mesh is soft and flexible, this can be impractical. The braiding along the hoop actuators will not transfer the forces to the immediately adjacent mesh before buckling. It would be advantageous to have the smallest initial angle possible that does not induce buckling.

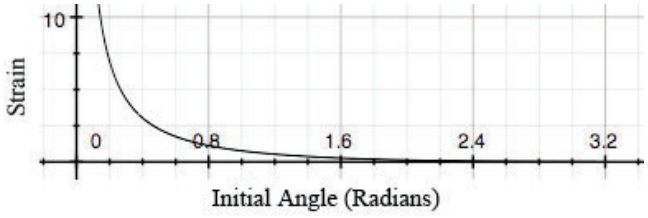

Figure 12: Strain as a function of the initial angle α, with a fixed displacement.

Despite the discontinuous nature of the simulated model, the analytical model can account for the problems discussed above. For a given robot design, the strain that is lost is typically the same over each step cycle, and can therefore be incorporated into the strain function by the subtraction of a constant value, Q:

$$P_{(t)} = \int_0^T (\varepsilon(t * V_{wave}) - Q)dt * V_{wave} \qquad (12)$$

The factor Q can be chosen such that the velocity, which is proportional to the strain curve, dips below zero at the first ground contact, and comes back up at lift off (Fig. 13, bottom). This is consistent with the observation that the strain that occurs after ground contact contributes to moving the robot backwards rather than forwards (Fig. 13, yellow shading). The area under the strain curve is also reduced substantially (Fig. 13, orange shading), thereby dramatically decreasing the displacement of the point on the robot. Even after the point has failed to fully utilize the strain at the beginning of the wave, it will lose again as the next segment has the same problem, and so on.

Figure 13 shows the position and velocity of a point on the simulated 2-D robot compared to the analytical model. One can see that the analytical model accurately predicts the

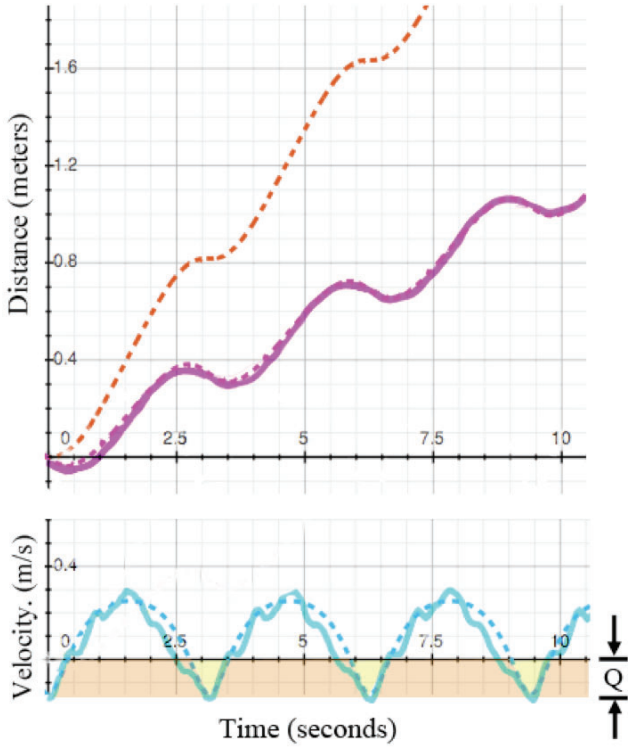

Figure 13: The position and velocity of a single point on the robot. The position is the integration of velocity over time, so the area shaded in orange is equal to the distance lost due to poor transitions between swing and stance. Solid lines are the simulation, while the dashed lines are the analytical model. The red dashed line is the position predicted by the analytical model if the robot has ideal swing-stance transitions and $Q = 0$.

robot position and velocity. The theoretical maximum speed is also shown, assuming the same robot was made from a continuously deforming mesh. This suggests that such a structure would have significant speed improvements over a discrete structure, even with ten segments.

The analytical model can provide many insights on its own. Adding more waves over the same length increases the number of ground contact points, and for this reason may create a more stable robot with better ground traction. *However, more waves come at the expense of a shorter step length, and alone cannot speed the robot up.* Faster speeds can only be achieved by building waveforms with higher strain rates, or by generating a faster wave. The shape of the waveform deformation is limited by the need to have ground contact, and to keep the forward moving sections from dragging on the ground. Above all, it is critical that the radially expanding segments do not contact the ground before they have fully expanded, and that radially contracting segments do not leave the ground before ground contact is established behind them. This will ensure that the critical strain change right after lift off is not lost and that the strain function remains positive at all times. These simple principles have greatly helped us focus our efforts for improving this method of locomotion.

VII. Conclusion

We found that our previous robot, and nearly all other robots that claim to use peristaltic motion, move much more slowly than predicted because of the kinematics and dynamics caused by very long actuators that greatly exaggerate the segmentation of the robot. Our study of the kinematics of peristaltic motion, both in simulation and using analytical tools, suggests a new design of a wormlike robot with a continuously deforming outer mesh.

We presented several methods of constructing such a robot with a continuously deforming exterior at different scales, and reported on the completion of a first prototype and its locomotion capabilities. By addressing the reliability of the mechanical design we will be able to further validate our understanding of peristaltic motion. This approach shows promise of great improvements of speed and performance over previous wormlike robotic platforms.

Acknowledgment

This work would not have been possible without the encouragement and support of many people, including Nicole Kern, Kenneth Loparo, and Andrew Horchler.

References

[1] B. A. Skierczynski, R. J. A. Wilson, W. B. Kristan, and R. Skalak, "A model of the hydrostatic skeleton of the leech," *J Theor Biol* 181:329–342, 1996.

[2] W. M. Kier and K. K. Smith, "Tongues, tentacles and trunks: the biomechanics of movement in muscular-hydrostats," *Zool J Linn Soc* 83:307–324, 1985.

[3] R. C. Brusca and G. J. Brusca, *Invertebrates*, Sinauer Associates, Sunderland, MA, 1990.

[4] S. Hirose, *Biologically Inspired Robots: Snake-Like Locomotors and Manipulators,* Oxford University Press, Oxford, 1993.

[5] A. J. Ijspeert, A. Crespi, D. Ryczko, and J. M. Cabelguen, "From swimming to walking with a salamander robot driven by a spinal cord model," *Science*, 315(5817):1416–1420, 2007.

[6] E. V. Mangan, D. A. Kingsley, R. D. Quinn, and H. J. Chiel, "Development of a peristaltic endoscope," *International Congress on Robotics and Automation (ICRA)*, 347–352, 2002.

[7] D. Trivedi,a, C. D. Rahn, W. M. Kier, and I. D. Walker, "Soft robotics: Biological inspiration, state of the art, and future research," *Applied Bionics and Biomechanics*, 5(3):99–117, Sep. 2003.

[8] A. Menciassi, S. Gorini, G. Pernorio, and P. Dario, "A SMA Actuated Artificial Earthworm," *International Congress on Robotics and Automation (ICRA)*, 2004.

[9] K. Zimmermann and I. Zeidis, "Worm-Like Motion as a Problem of Nonlinear Dynamics," *Journal of Theoretical and Applied Mechanics*, 45(1):179–187, 2007.

[10] H. Omori, T. Hayakawa and T. Nakamura, "A Peristaltic Crawling Earthworm Robot Composed of Flexible Units," *International Conference on Intelligent Robots (IROS)*, 2008.

[11] B. Trimmer, A. Takesian, and B. Sweet.,"Caterpillar locomotion: a new model for soft-bodied climbing and burrowing robots," *7th International Symposium on Technology and the Mine Problem*, Monterey, CA, 2006.

[12] M. Ingram and D. Hong, "Whole Skin Locomotion Mechanism Inspired by Amoeboid Motility Mechanisms," *IDETC/CIE*, 2005.

[13] R. D. Quinn, G. M. Nelson, R. E. Ritzmann, R. J. Bachmann, D. A. Kingsley, J. T. Offi, and T. J. Allen, "Parallel Strategies for Implementing Biological Principles Into Mobile Robots," *Int. Journal of Robotics Research*, 22(3):169–186, 2003.

[14] K. J. Quillin, "Kinematic scaling of locomotion by hydrostatic animals: ontogeny of peristaltic crawiling by the earthworm lumbricusterrestris," *The Journal of Experimental Biology*, 202:661–674, 1999.